Journal of
Materials Chemistry A

Accepted Manuscript

This article can be cited before page numbers have been issued, to do this please use: T. A. Makal, W. Zhuang and H. Zhou, *J. Mater. Chem. A*, 2013, DOI: 10.1039/C3TA12761C.

This is an *Accepted Manuscript*, which has been through the RSC Publishing peer review process and has been accepted for publication.

Accepted Manuscripts are published online shortly after acceptance, which is prior to technical editing, formatting and proof reading. This free service from RSC Publishing allows authors to make their results available to the community, in citable form, before publication of the edited article. This *Accepted Manuscript* will be replaced by the edited and formatted *Advance Article* as soon as this is available.

To cite this manuscript please use its permanent Digital Object Identifier (DOI®), which is identical for all formats of publication.

More information about *Accepted Manuscripts* can be found in the **Information for Authors**.

Please note that technical editing may introduce minor changes to the text and/or graphics contained in the manuscript submitted by the author(s) which may alter content, and that the standard **Terms & Conditions** and the **ethical guidelines** that apply to the journal are still applicable. In no event shall the RSC be held responsible for any errors or omissions in these *Accepted Manuscript* manuscripts or any consequences arising from the use of any information contained in them.

Journal of Materials Chemistry A

View Article Online
DOI: 10.1039/C3TA12761C

Journal of Materials Chemistry A

Dynamic Article Links

Cite this: DOI: 10.1039/c0xx00000x

ARTICLE

www.rsc.org/xxxxxx

Realization of both high hydrogen selectivity and capacity in a guest responsive metal-organic framework†

Trevor A. Makal‡, Wenjuan Zhuang, Hongcai Zhou*[a]

Received (in XXX, XXX) Xth XXXXXXXXX 20XX, Accepted Xth XXXXXXXXX 20XX

DOI: 10.1039/b000000x

Two newly designed semi-flexible tetratopic carboxylate ligands, 5',5""-(propane-2,2-diyl)bis(2'-methoxy-[1,1':3',1"-terphenyl]-4,4"-dicarboxylate) (pbtd-OMe^{4-}) and 5',5""-(propane-2,2-diyl)bis(2'-ethoxy-[1,1':3',1"-terphenyl]-4,4"-dicarboxylate) (pbtd-OEt^{4-}) have been used to connect dicopper paddlewheel building units to afford two isostructural metal-organic frameworks, $Cu_2(H_2O)_2$(pbtd-OR)·*x*S (R = Me, PCN-38·*x*S; R = Et, PCN-39·*x*S, *S* represents noncoordinated guest molecules, PCN = porous coordination network) with novel structure and gas sorption properties upon activation. PCN-39 undergoes structural transformations upon guest solvent removal, leading to observation of distinct phases from *in situ* powder X-ray diffraction measurements, and exhibits selective adsorption of H_2 (up to 2.0 wt%) over CO, CO_2, and N_2, which can be explained by optimized space-filling of the pendant ethoxy group. PCN-38 undergoes no transformation upon activation and exhibits hydrogen uptake up to 2.2 wt%, as well as moderate uptake of other gases. The selective adsorption of hydrogen over other gases highlights the potential application of PCN-39 in industrially important gas separation.

Introduction

Metal-organic frameworks (MOFs)[1-5] have received an incredible following over the past 20 years owing to their exceptionally high surface areas, large pore volumes, tunable surfaces, and potential applications in such areas as gas storage,[6-12] gas/vapor separations,[13-16] heterogeneous catalysis,[17-22] chemical sensing,[23-27] biomedical applications,[28-30] and stimuli-responsive materials.[31-33] The potential for their use in commercial applications is largely dictated by a number of factors, including surface area and micropore volume, in addition to functionalities based upon structural design and functional groups, and stability. In particular, the synthesis of porous MOFs with responsive modification of pore sizes is of great interest in the area of selective gas sorption and separations. To make effective materials for separation processes, the pore surface characteristics must be tuned appropriately so as to create a sieving effect, where molecules are separated based upon physical characteristics, or through inclusion of polar or charged functional groups to take advantage of chemical differences between molecules.[34, 35] Recently, Schröder, Yang, and coworkers reported a dynamic bifunctional MOF for the selective adsorption of CO_2 over acetylene.[36] From *in situ* powder X-ray diffraction studies, they were able to observe a structural transformation from a "narrow pore" to a "large pore" conformation upon CO_2 loading attributed to a gating effect by pendant pyridyl groups. In addition to playing a role in gate-opening phenomena, we have been interested in investigating the roles of pendant groups on the crystallization and gas sorptive properties of MOFs. Furthermore, few porous materials have been shown to preferentially adsorb H_2 over N_2, and those that do exhibit high selectivity toward H_2 typically do so in low capacities.[8, 37]

Since it is well known that the filling of void space within a system is of considerable importance to the formation and stability of porous frameworks,[38-40] we have been investigating the consequence of pendant functional groups on the formation and gas sorption properties of MOFs. By grafting pendant functionalities on non-rigid (semi-flexible) ligands, the ability of pendant groups to initiate structural changes in the framework system through optimal filling of void space may be investigated. To this end, we synthesized the two angular, tetratopic ligand precursors H_4pbtd-OMe and H_4pbtd-OEt (H_4pbtd-OMe = 5',5""-(propane-2,2-diyl)bis(2'-methoxy-[1,1':3',1"-terphenyl]-4,4"-dicarboxylic acid), H_4pbtd-OEt = 5',5""-(propane-2,2-diyl)bis(2'-

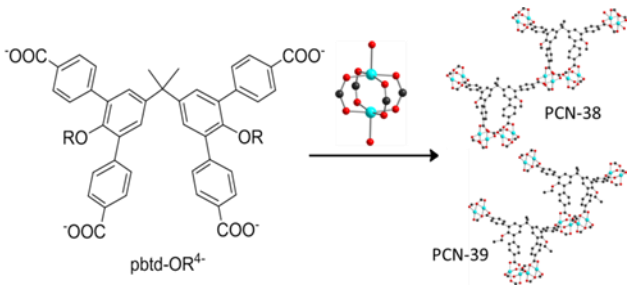

Fig. 1 Schematic representation of the coordination environments of pbtd-OR^{4-} and dicopper(II) paddlewheel SBUs in PCN-38 (R=Me) and PCN-39 (R=Et).

View Article Online
DOI: 10.1039/C3TA12761E

ethoxy-[1,1':3',1"-terphenyl]-4,4"-dicarboxylic acid)) and report the resultant MOFs obtained from combination with dicopper paddlewheel SBUs (Figure 1).

The ligands share the same core structure as the organic linker reported in the formation of PCN-21,[41] with the addition of pendant methyl and ethyl ether linkages in the para-positions of the central phenyl rings that are joined by a methylene bridge and two methyl groups on the bridging methylene carbon atom. The two reported MOFs, however, do not resemble the highly porous and highly symmetric PCN-21, likely due to the factors described in the following sentences. The methylene bridge in each ligand permits a level of flexibility that allows for minor structural movement to minimize the energy of the systems, and, along with the extension of pendant ether moieties, leads to systems that reorganize to optimally fill space. This combination of properties has led to interesting crystallographic and gas sorption properties of the reported MOFs. The rearrangement of pore space within PCN-39 realizes a molecular sieving effect in which no gases larger than hydrogen in this study may be adsorbed and, unlike many previously reported materials with high H_2 selectivity, also exhibits high H_2 storage capacity. This combination of properties shows great potential for application in hydrogen purification applications.

Experimental Section

General Information. Commercially available reagents were used as received without further purification. Nuclear magnetic resonance (NMR) ^{1}H data were collected on a 300 MHz Mercury 300 spectrometer. Thermogravimetric analyses (TGA) were performed under N_2 flow on a Shimadzu TGA-50 thermogravimetric analyzer with a heating rate of 5 ˚C min^{-1}.

*Synthesis of 5',5'''' - (propane - 2,2 - diyl)bis(2' –methoxy - [1,1':3',1'' - terphenyl] - 4,4'' - dicarboxylic acid, (H_4pbtd-OMe) and 5',5'''' - (propane - 2,2 - diyl)bis(2' – ethoxy - [1,1':3',1'' - terphenyl] - 4,4'' - dicarboxylic acid, (H_4pbtd-OEt). a. 5,5' - (propane - 2,2 - diyl)bis(1,3 –dibromo - 2 - methoxybenzene) (**A**).* This compound was synthesized following a procedure similar to a literature method.[42] Tetrabromobisphenol A (5.44 g, 10 mmol) and K_2CO_3 (5.2 g, 37.6 mmol) were combined in a 250 mL Schlenk flask equipped with magnetic stirrer and air condenser. The flask was purged under vacuum and refilled with N_2 three times, and then 120 mL dry *N,N*-dimethylformamide (DMF) was added *via* canula. Methyl iodide (2.5 mL, 40.0 mmol) was then added to the reaction flask by syringe. The reaction mixture was stirred and heated at reflux under nitrogen atmosphere overnight. After cooling to room temperature, the solution was poured over ice-water. The resultant white solid was collected by vacuum filtration then dissolved in ethyl acetate, washed with water and brine, then dried over $MgSO_4$. Evaporation of organic solvent yielded 5.33 g (93.3%) **A** as colorless crystals. ^{1}H NMR (300 MHz, $CDCl_3$): δ 7.29 (s, 4H), 3.78 (s, 6H), 1.54 (s, 6H).

*b. Tetramethyl 5',5'''' - (propane - 2,2 - diyl)bis(2' –methoxy - [1,1':3',1'' - terphenyl] - 4,4'' - dicarboxylate (**B**).* Compound **A** (2.00 g, 1.14 mmol), 4-(methoxycarbonyl)phenylboronic acid (4.40 g, 24.4 mmol), CsF (2 g, 13 mmol), and $Pd(PPh_3)_4$ (0.20 g, 0.4 mmol) were mixed in a 500 mL Schlenk flask equipped with magnetic stirrer and air condenser. The flask was purged under vacuum and backfilled with N_2 three times, and then degassed. 1,2-dimethoxyethane (DME, 200 mL) was added *via* canula. The reaction mixture was stirred and heated at reflux under nitrogen atmosphere. The reaction was monitored by thin-layer chromatography (1:4 by volume ethyl acetate:hexanes as eluent). After removal of organic solvent, the resultant solid was dissolved in dichloromethane, washed with water and brine, dried over MgSO4, filtered, and reduced *in vacuo* yielding 0.5 g (55.3 %) **B** as a white powder. ^{1}H NMR (300 MHz, $CDCl_3$): δ 8.08 (d, 8H), 7.67 (d, 8H), 7.28 (s, 4H), 3.95 (s, 12H), 3.12 (s, 6H), 1.80 (s, 6H).

c. H_4pbtd-OMe. Compound **B** (0.5 g, 0.6 mmol) was suspended in 120 mL tetrahydrofuran/methanol/water mixture (1:1:1 by volume), to which 6 g KOH was added. The mixture was stirred at 60 °C overnight. Organic solvents were removed *in vacuo* and the aqueous solution acidified with 20% aqueous hydrochloric acid until the pH value was adjusted to approximately 2. The resulting white precipitate was collected by vacuum filtration, washed with water, and dried in an oven to yield 0.28 g (63.3 %) H_4pbtd-OMe. ^{1}H NMR (300 MHz, DMSO-d^6): δ 12.98 (br, 4H), 7.97 (d, 8H), 7.66 (d, 8H), 7.33 (s, 4H), 3.04 (s, 6H), 1.80 (s, 6H).

*d. 5,5' - (propane - 2,2 - diyl)bis(1,3 – dibromo – 2 - ethoxybenzene), (**C**).* Tetrabromobisphenol A (5.44 g, 10 mmol) and K_2CO_3 (5.2 g, 37.6 mmol) were combined in a 250 mL Schlenk flask equipped with magnetic stirrer and air condenser. The flask was purged under vacuum and refilled with N2 three times, and then 60 mL dry DMF was added *via* canula. Degassed ethyl bromide (3.8 mL, 51.8 mmol) was then added to the reaction flask by syringe. The reaction mixture was stirred and heated at reflux under nitrogen atmosphere for 24 hours. After cooling to room temperature, the solution was poured over ice-water, yielding 5.40 g (90.5 %) **C** as a fine white powder, which was collected by vacuum filtration and dried in an oven. ^{1}H NMR (300 MHz, $CDCl_3$): δ 7.29 (s, 4H), 4.07 (q, 4H), 1.59 (s, 6H), 1.48 (t, 6H).

*e. Tetramethyl 5',5'''' - (Propane - 2,2 - diyl)bis(2' -ethoxy - [1,1':3',1'' - terphenyl] - 4,4'' - dicarboxylate, (**D**).* Compound **C** (2.51 g, 4.2 mmol), 4-(methoxycarbonyl)phenylboronic acid (4.50 g, 25.0 mmol), CsF (2.5 g, 16.25 mmol), $NaHCO_3$ (1.25 g, 14.9 mmol), and Pd(PPh3)4 (0.19 g, 0.4 mmol) were mixed in a 500 mL Schlenk flask equipped with magnetic stirrer and air condenser. The flask was purged under vacuum and refilled with N_2 three times, and then a mixture of degassed 1,2-dimethoxyethane (150 mL) and water (20 mL) was added *via* canula. The reaction mixture was stirred and heated at reflux under nitrogen atmosphere. The reaction was monitored by thin-layer chromatography (1:4 by volume ethyl acetate:hexanes as eluent). After removal of organic solvent *in vacuo*, the aqueous layer was extracted with dichloromethane (100 mL, 3x), dried over $MgSO_4$, filtered, and reduced *in vacuo*. The mixture of products was separated by column chromatography using a silica gel column and reduced to afford 0.51 g (14.8 %) **D**. ^{1}H NMR (300 MHz, $CDCl_3$) δ 8.08 (d, 8H), 7.65 (d, 8H), 7.27 (s, 4H), 3.94 (s, 12H), 3.20 (q, 4H), 1.79 (s, 6H), 0.76 (t, 6H).

f. H_4pbtd-OEt. Compound **D** (0.51 g, 0.6 mmol) was suspended in 60 mL tetrahydrofuran/methanol mixture (1:1 by volume), to which 10 mL 5 M NaOH solution was added. The mixture was stirred at room temperature overnight, and then

View Article Online
DOI: 10.1039/C3TA12761C

heated at reflux until no starting material was observed by TLC. Organic solvents were removed *in vacuo* and the aqueous solution acidified with 20% aqueous hydrochloric acid until the pH value was adjusted to approximately 2. The resulting white precipitate was collected by vacuum filtration, washed with water, and dried in an oven to yield H_4pbtd-OEt in quantitative yield. ^{1}H NMR (300 MHz, DMSO-d^6): δ 12.98 (br, 4H), 7.98 (d, 8H), 7.70 (d, 8H), 7.35 (s, 4H), 3.19 (q, 4H), 1.81 (s, 6H), 0.70 (t, 6H).

Synthesis of PCN-38·xS, $Cu_2(H_2O)_2$(pbtd-OMe)·xS. To a 2 mL glass vial was added 0.005 g (0.0068 mmol) H_4pbtd-OMe and 0.015 g (0.064 mmol) $Cu(NO_3)_2 \cdot 2.5\ H_2O$ dissolved in 1.5 mL *N*,*N*-dimethylacetamide (DMA) with 4 drops HBF_4 (48% min w/w aqueous solution). The reaction was kept at 85 °C in an oven for 72 h. The resulting blue-teal crystals of $Cu_2(H_2O)_2$(pbtd-OMe)·*xS* (PCN-28·*xS*, *S*=noncoordinated solvent molecule) were then decanted, washed with fresh DMA, and collected.

Synthesis of PCN-39·xS, $Cu_2(H_2O)_2$(pbtd-OEt)·xS. To a 2 mL glass vial was added 0.005 g (0.0065 mmol) H_4pbtd-OEt and 0.015 g (0.064 mmol) $Cu(NO_3)_2 \cdot 2.5\ H_2O$ dissolved in 1.5 mL *N*,*N*-dimethylacetamide (DMA) with 4 drops HBF_4 (48% min w/w aqueous solution). The reaction was kept at 85 °C in an oven for 72 h. The resulting blue-teal crystals of $Cu_2(H_2O)_2$(pbtd-OEt)·*xS* (PCN-29·*xS*, *S*=noncoordinated solvent molecule) were then decanted, washed with fresh DMA, and collected.

X-ray Crystallography. Single crystal X-ray diffraction (XRD) measurements were performed on a Bruker SMART APEXii diffractometer equipped with CCD detector, an Oxford Cryostream low temperature device, and a fine-focus sealed-tube X-ray source (Mo-Kα radiation, λ = 0.71073 Å, graphite monochromated) operating at 50 kV and 30 mA. Raw data collection and refinement were performed using SMART. Absorption corrections were applied using the *SADABS* routine. The structures were solved through direct methods and refined by full-matrix least-squares on F^2 with anisotropic displacement using *SHELXTL*.[43] Non-hydrogen atoms were refined with anisotropic displacement parameters during the final cycles. Hydrogen atoms on carbon were calculated in ideal positions with isotropic displacement parameters set to 1.2 x U_{eq} of the attached atom. Solvent molecules in the structures were highly disordered and attempts to locate and refine solvent peaks were unsuccessful. Therefore, the contribution of solvent electron density was removed by the *SQUEEZE* routine in *PLATON* and refined further using the data generated.[44] The contents of the solvent region are not represented in the unit cell contents in the crystal data. The details for data collection and refinement are included in the CIF files in the Supporting Information.

Powder X-ray diffraction (PXRD) patterns were collected on a Bruker D8-Focus Bragg-Brentano X-ray Powder diffractometer equipped with a Cu sealed tube (λ = 1.54178 Å) and graphite monochromator at a scan rate of 1 s deg^{-1}, solid state detector, and a routine power of 1600 W (40 kV, 40 mA). The samples were dispersed on Si single crystal zero diffraction plate for analysis. Simulation of the PXRD pattern was carried out by the single-crystal data and diffraction-crystal module of the *Mercury* program available free-of-charge via internet at http://www.ccdc.cam.ac.uk/products/mercury/. Full pattern decomposition was performed using the *Jana2006* program available free of charge at http://www-xray.fzu.cz/jana/jana.html. *Ex situ* TGA/PXRD experiments were conducted by heating a fresh sample of PCN-39 to 348 K, 379 K, 393 K, or 412 K at a rate of 10 ˚C/min, allowing the sample to cool to room temperature in a nitrogen atmosphere, then transferring to a Si single crystal zero diffraction plate and the X-ray diffraction pattern collected.

Three separate *in situ* X-ray powder diffraction studies were performed on Beamline 1-BM-C at the Advanced Photon Source at Argonne National Laboratory: heating-cooling under closed system, heating-cooling under He flow, and flowing He under isothermal conditions.

For the heating-cooling cycle under closed system, a fresh sample of PCN-39 was transferred to a capillary tube, and then introduced to a flow cell with both input and output valves closed. The sample was heated from 295 – 473 K at a rate of 2 K/min, maintained at 473 K for 30 min, and then quickly cooled to room temperature while collecting diffraction data. The heating-cooling cycle under He flow was conducted by transferring a fresh sample of PCN-39 to a capillary tube, then introducing the sample filled capillary to a flow cell connected to He source. The input and output valves remained open during the experiment so as to allow fresh He to flow over the sample while heating from 295 – 473 K at a rate of 3 K/min, maintaining the temperature at 473 K for 30 min, and then cooling to 295 K at a rate of 3 K/min. The isothermal experiment was conducted in a similar manner as the previous experiment, but with maintaining the temperature at 295 K with continuous He flow overnight. For each diffraction pattern, the sample was exposed to synchrotron X-ray radiation (λ = 0.60570 Å) 20 times over 6 sec, rocking the sample +/- 5˚ to reduce artifacts from non-monodisperse particle sizes.

Low-Pressure Gas Adsorption Measurements. Gas sorption isotherm measurements were performed on ASAP 2020 and ASAP 2420 Surface Area and Pore Size Analyzers. As-synthesized samples of PCN-38·*xS* and PCN-39·*xS* were immersed in dry methanol for 24 h and the extract decanted. Fresh dry methanol was subsequently added and the crystals remained in the solvent for an additional 24 h. Each sample was collected by decanting and the procedure repeated once more with dry methanol, and three subsequent times with dry dichloromethane. After the removal of dichloromethane by decanting, the samples were activated by drying under a dynamic vacuum at room temperature and at 75 °C overnight to produce activated samples of PCN-38 and -39 (PCN-38(ac) and PCN-39(ac)). Before the measurement, PCN-38 was again further activated using the "degas" function of the surface area analyzer for 4 h at 60 °C, and PCN-39 for 5 h at 80 °C. Other activation temperatures were tested, with the reported methods providing the best sorption properties. UHP grade (99.999%) N_2, H_2, CO_2, CO, and CH_4 were used for all measurements.

Results and Discussion

Syntheses and Structures of PCN-38·*xS* and PCN-39·*xS*.[#] Under solvothermal conditions, reactions between $Cu(NO_3)_2 \cdot 2.5\ H_2O$ and H_4pbtd-OR in DMA afforded teal-blue crystals of PCN-38·*xS* (R = Me) and PCN-39·*xS* (R = Et), which has a formula of $Cu_2(H_2O)_2$(pbtd-OR)·*xS*. Single-crystal XRD analyses revealed

Cite this: DOI: 10.1039/c0xx00000x

ARTICLE

www.rsc.org/xxxxxx

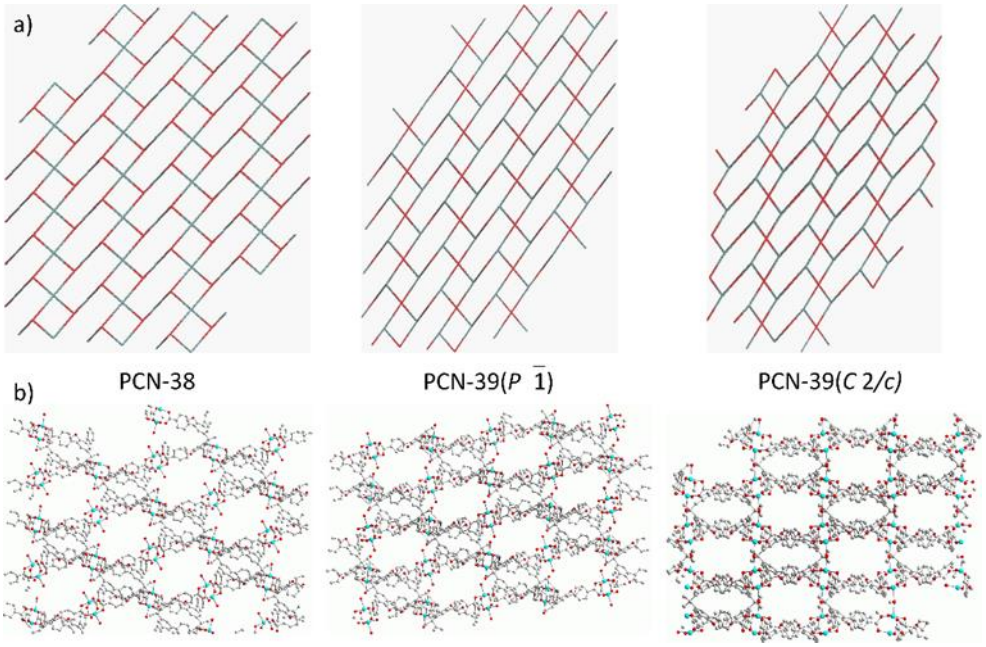

Fig. 2 (a) View of the distorted PtS nets of PCN-38, PCN-39($P\ \bar{1}$), and PCN-39($C\ 2/c$). (b) View along topologically equivalent directions in PCN-38 (left), PCN-39($P\ \bar{1}$) (middle), and PCN-39($C\ 2/c$) (right) illustrating the difference in alignment of dicopper paddlewheels. The change in alignment of Cu_2-SBUs upon activation of PCN-39 leads to a redistribution of pore sizes and selective adsorption of H_2. Cu = turquoise; C = grey; O = red; H and coordinated solvent excluded, for clarity.

that PCN-38 crystallizes in the triclinic space group $P\ \bar{1}$ with unit cell parameters a=20.639, b=23.923, c=23.247 Å, α=82.718, β=71.061, and γ=80.352° (CCDC-950465). Two separate phases of PCN-39 were identified through single-crystal XRD studies, one which crystallizes in the triclinic space group $P\ \bar{1}$ with unit cell parameters a=15.021, b=16.620, c=19.295 Å, α=102.288, β=91.786, and γ=93.300° , denoted PCN-39($P\ \bar{1}$) (CCDC-950464), and one which crystallizes in the monoclinic space group $C\ 2/c$ with unit cell parameters a=20.530, b=20.773, c=18.804 Å, β=90.945°, denoted PCN-39($C\ 2/c$) (CCDC-950392).

In PCN-38, two Cu_2-paddlwheel SBUs connect to two pbtd-OMe^{4-} ligands to construct a three-dimensional porous framework with solvent accessible volume of 70.7% (calculated using *PLATON*),[44] and open pores with dimension 6 × 7 $Å^2$ along the [1 0 1] direction and two types of pores along the [0 1 1] direction, 6 × 24 $Å^2$ and 8 × 9 $Å^2$ (atom to atom distances minus van der Waals radii). The asymmetric unit in PCN-39($P\ \bar{1}$) consists of two Cu(II) ions and one pbtd-OEt^{4-} ligand. The inversion center in PCN-39($P\ \bar{1}$) lies in the middle of one of the dicopper paddlewheels, such that there are two crystallographically distinct Cu(II) ions in the asymmetric unit that make up two distinct dicopper paddlewheel building units. The solvent accessible volume in PCN-39($P\ \bar{1}$), as calculated using *PLATON*, is 66.1%. Whereas PCN-39($C\ 2/c$) consists of one Cu(II) ion and half of the pbtd-OEt^{4-} ligand, owing to the higher symmetry of the framework. The solvent accessible volume is 60.2%. Topologically, when considering the dicopper paddlewheel and ligand as 4-connected nodes, each framework possesses a distorted *pts* net with the point (Schläfli) symbol $[4^2{\cdot}8^4]$ and vertex symbol [4.4.8(7).8(7).8(7).8(7)] [4.4.8(2).8(2).8(8).8(8)] calculated with the *TOPOS* software package, Figure 2.

The most obvious difference between PCN-39($P\ \bar{1}$) and PCN-39($C\ 2/c$) is in the alignment of dicopper paddlewheels, which leads to a redistribution of pore sizes between the two phases. The largest channels in PCN-39($P\ \bar{1}$) are accessible from pore openings of 4.0 Å, whereas PCN-39($C\ 2/c$) contains openings only as large as 3.0 Å. PCN-38 and -39 were observed to be stable over 260 °C, from thermogravimetric analyses (Figure S5).

The pbtd-OR^{4-} ligands are considered "semi-flexible" due to the sp^3-hybridized carbons connecting the isopthalate moieties that allow for flexibility in the central bond angle. The pendant alkyl groups bound to the 4-position of the tetrasubstituted phenyl rings are believed to play a role in stabilizing the frameworks by filling void space within the pores of the system. This appears to be more significant for the framework with longer pendant group, PCN-39, and is believed to be the genesis of the observed structural changes in the MOF (see Figure S6 and Table S1 for overlay of ligands in PCN-39($P\ \bar{1}$) and -39($C\ 2/c$)).

View Article Online
DOI: 10.1039/C3TA12761C

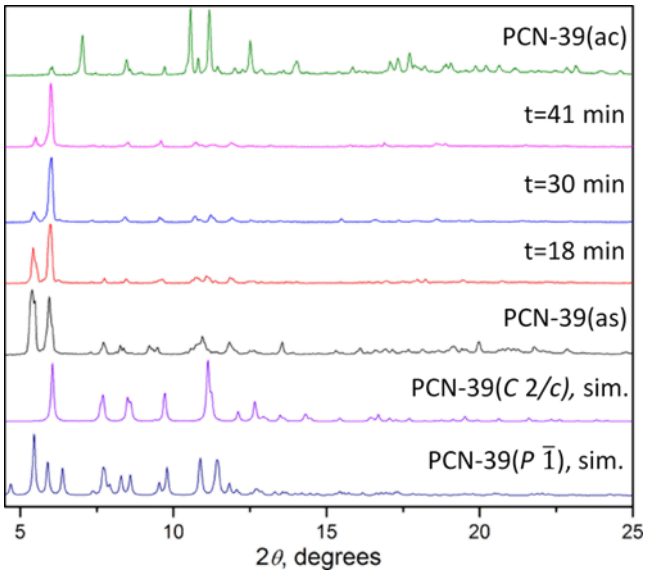

Fig. 3 PXRD patterns of PCN-39 upon exposure to atmospheric conditions for time, t, compared to simulated patterns of PCN-39(*C* 2/*c*) and -39(*P* $\bar{1}$) from single crystal XRD data. PCN-39(as) exposed to air <1 min before collecting PXRD pattern; (as) = as-synthesized, (ac) = activated sample.

Importantly, in both triclinic systems, PCN-38 and -39(*P* $\bar{1}$), there are observed methyl-methyl close contacts between methyl groups extending from the central methylene bridges on nearby linkers (3.774(5) and 3.744(6) Å C-C distances, respectively). PCN-39(*C* 2/*c*), however, increases the separation between these central methyl groups to 7.143(0) Å due to redistribution of pore sizes (Figure S7).

Thermogravimetric analyses indicate a mass loss of ~31% for both materials up to 250 °C. This relates to a loss of one coordinated water molecule and ~2 DMA molecules for each copper ion.

Structural transformation of PCN-39. Bulk samples of PCN-39 were synthesized and evaluated by Le Bail full pattern decomposition with initial unit cell parameters and space groups obtained from single-crystal XRD data (Figures S8-S11). Bulk samples of as-synthesized PCN-39 were determined to be predominantly PCN-39(*P* $\bar{1}$) upon initial characterization, with subsequent measurements showing significant increase in the presence of PCN-39(*C* 2/*c*) and decrease of PCN-39(*P* $\bar{1}$) upon extended exposure to air, Figure 3. Additionally, a fresh sample of PCN-39 was exchanged with methanol and dried at room temperature under dynamic vacuum for 1 h and PXRD measured, showing complete disappearance of the original PCN-39(*P* $\bar{1}$) phase with conversion to the PCN-39(*C* 2/*c*) phase. Since PCN-39(*P* $\bar{1}$) quickly loses solvent and subsequently undergoes structural transformation, a fresh sample of PCN-39 was removed from the mother liquor and excess solvent removed from the surface of the crystalline powder by transferring to a filter paper before introducing the sample to a Si single crystal zero diffraction plate (< 1 min exposure to air) for PXRD analysis. The PXRD measurement was repeated another 3 times after the original measurement, one after another, the most significant observation being a shift in the relative intensities of the first two reflections at $2\theta \approx 5.5^\circ$ (corresponding to PCN-39(*P* $\bar{1}$)) and 6.0° (present in both PCN-39(*P* $\bar{1}$) and PCN-39(*C* 2/*c*)). Furthermore, upon exchanging the larger, high boiling point solvent (DMA)

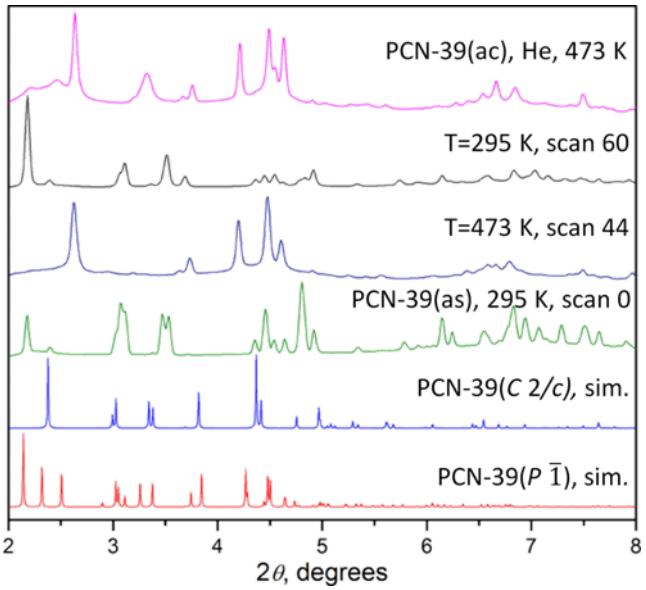

Fig. 4 *In situ* synchrotron PXRD patterns of PCN-39 upon heating in a closed system at temperature, T, compared to PXRD patterns of PCN-39(*P* $\bar{1}$) and -39(*C* 2/*c*) simulated from single crystal data, and PCN-39(ac) activated in He stream.

with a smaller guest species (methanol or dichloromethane), the same structural transformation is observed.

The observed structural transformation may be described as a reorganization of the bound ligand to a more symmetric, lower energy conformation. We propose that the removal of excess DMA molecules from the open channels of the system or exchange of DMA for smaller guests promotes the relaxation of the framework to allow pendant ethoxy groups to minimize empty space within the system. Based on the observations of quick transformation upon removal of PCN-39(as) from the mother liquor, it can be deduced that the monoclinic form is considerably favorable over the triclinic form, resulting in the "squeezing" of excess DMA molecules from the pores. A similar transformation is not observed for PCN-38 likely because the pendant methoxy groups on pbtd-OMe^{4-} do not possess the same degree of flexibility as ethoxy groups, nor occupy as much free volume.

To further probe the structural transformation process PCN-39 was analyzed by *in situ* PXRD. A freshly prepared sample was transferred to a capillary tube and enclosed in a closed system, then heated from 295 K to 473 K and cooled to 295 K while collecting diffraction patterns. Four distinct transformations in the crystal structure were observed from the *in situ* diffraction study, Figure 4. The first phase observed (PCN-39(as)) is predominantly that of PCN-39(*P* $\bar{1}$) and is present from 295 – 375 K (Figure S12). A transition occurs from 375 – 379 K, resulting in a mixture of PCN-39(*P* $\bar{1}$) and PCN-39(*C* 2/*c*) (Figure S13). From 383 – 404 K a phase or mixture of unknown structure is observed, and transitions into a second, distinct phase or mixture of unknown structure (activated phase) that remains from 412 K – 473 K. Upon cooling, the DMA in the closed system condensed and resulted in transformation from the activated phase back to the originally observed PCN-39(as) (predominantly PCN-39(*P* $\bar{1}$) species) at 295 K with no apparent loss of crystallinity

View Article Online
DOI: 10.1039/C3TA12761E

(Figure S14).

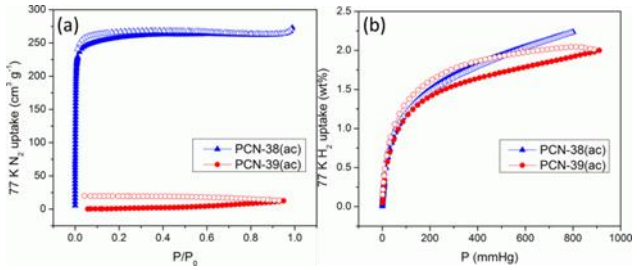

Fig. 5 (a) N_2 and (b) H_2uptake of PCN-38(ac) and -39(ac) at 77 K. Solid symbols represent adsorption and open symbols desorption.

Attempts to isolate individual phases at each of the transitions were performed *via ex situ* TGA/PXRD experiments. However, only two separate phases were isolated, in addition to the initial predominantly PCN-39($P\ \bar{1}$) phase. The first was isolated from heating a fresh sample of PCN-39 to 348 K, and, as expected, corresponds to predominantly PCN-39(C 2/c). Heating fresh samples of PCN-39 to 379 K, 393 K, and 412 K all resulted in the isolation of material of the same crystalline phase with unknown structure (Figure S15).

The *in situ* PXRD experiment conducted under He flow showed isolation of the activated phase at 473 K, and retained its crystallinity in the activated form upon lowering the temperature back to 295 K, Figure 4. Unlike the closed system experiment, the He stream carries away all evaporated DMA, eliminating the possibility of reintroduction to the pores which facilitates the structural transformation back to PCN-39(as). The fully activated sample is shown to be stable in inert atmosphere, and retains crystallinity.

Gas sorption. To investigate the permanent porosity of PCN-38 and PCN-39, gas sorption experiments evaluating N_2, H_2, CO_2, CO, and CH_4 uptake were performed. The freshly prepared samples of PCN-38 and PCN-39 were first solvent exchanged with methanol, then dichloromethane, resulting in a color change from teal in DMA, to green in methanol, to blue in dichloromethane, and finally deep purple upon activation, typical of dicopper(II)-paddlewheel frameworks. The N_2 sorption isotherms, Figure 5a, reveal that PCN-38(ac) exhibits typical Type I sorption behavior, a characteristic of microporous materials,[45] which is congruent with the crystal structure. PCN-38(ac) exhibits moderate N_2 uptake at 1 bar and 77 K (*ca*. 270 $cm^3\ g^{-1}$). By applying the BET model, the apparent surface area is estimated to be ~911 $m^2\ g^{-1}$ (1134 $m^2 g^{-1}$ Langmuir). At 77K and 1 bar, PCN-38(ac) adsorbs a reasonably high amount of H_2, 2.2 wt%, Figure 5b , comparable to the MOF Zn_2(btbz), which possesses similar surface area and H_2 uptake capacity.[46] PCN-39(ac) also adsorbs moderate amounts of CH_4, CO_2, O_2, and Ar (Figures S16 and S17).

PCN-39(ac), however, undergoes a redistribution of pore sizes (PCN-39($P\ \bar{1}$) to -39(C 2/c) and likely further) during the activation process that precludes the adsorption of N_2 into the pores. Instead, PCN-39(ac) adsorbs up to 2.0 wt% H_2 (kinetic diameter 2.89 Å) selectively over CO (3.69 Å), N_2 (3.64 Å), and CO_2 (3.30 Å) (Figure S18). The observed hysteresis in the H_2 isotherm is attributed to flexibility in the system, resulting in a tight fitting of the dihydrogen molecules in the pores and retention of H_2 guests at lower pressures. The flexibility of the pendant –OEt group along with the central sp^3-hybridized carbon is proposed to allow for optimal filling of empty space within the pores upon activation by shifting its conformation to eliminate "dead volume" as larger guest molecules are removed, forming a vacuum. This guest responsive transformation plays a role in stabilizing the framework and reduces the size of pore apertures, creating pores accessible only to H_2 and smaller guests. The inability of PCN-39 to adsorb any gas larger than H_2 reveals the role of the pendant ethoxy group in blocking the accessible pores and lends this system to application in pre-combustion hydrogen purification. While PCN-39 performs about average as a H_2 storage medium, compared to other reported porous materials, the significant selectivity of the framework toward H_2 over CO_2, N_2, and CO highlights the potential of this material to serve in pre-combustion hydrogen purification systems.

Conclusions

In this report, two isostructural metal-organic frameworks (PCN-38 and -39) have been synthesized with tetratopic ligands featuring pendant alkoxy groups with semi-flexible backbones. From PCN-38 to -39, the framework is instilled with guest responsive properties by replacing methoxy groups on the central phenyl rings with ethoxy groups. The increased length and flexibility of the ethoxy groups induce structural transformations upon guest removal and activation through optimized space-filling of the evacuated pores. This feature leads to H_2 adsorption capacity up to 2.0 wt% at 77 K and 1 bar, and selectivity over N_2, CO, and CO_2 in PCN-39. Whereas, PCN-38, with shorter methoxy pendant group, undergoes no such structural transformation and adsorbs CO, CO_2, N_2, and H_2 (2.2 wt% at 77 K and 1 bar). The structural transformations of PCN-39 were monitored *via in situ* PXRD measurements and the integrity of the crystalline framework confirmed upon desolvation, returning full-circle to the original framework after heating and cooling in a closed system. This work is a successful demonstration of the role of pendant alkoxy groups in minimizing framework energy and forming guest (stimuli) responsive materials capable of selectively adsorbing H_2 over other gases. This result improves upon previous efforts at selective adsorption of H_2 over N_2 for such applications as isolation of H_2 from ammonia synthesis waste streams.[47, 48] Further studies will focus on exploring pendant alkoxy groups to design gate-opening and water stable MOFs.

Notes and references

[a] *Department of Chemistry, Texas A&M University, College Station, TX 77840 (USA). Fax: (+1) 979-845-1595; Tel: (+1) 979-845-4034; E-mail: zhou@chem.tamu.edu*

‡ *Current address: Department of Natural Sciences, The University of Virginia's College at Wise, Wise, VA 24293 (USA).*

† Electronic Supplementary Information (ESI) available: NMR spectra, thermogravimetric analyses, PXRD and Le Bail fits for PCN-39($P\ \bar{1}$) and -39(C 2/c), overlay of conformations of ligand in PCN-39($P\ \bar{1}$) and -39(C 2/c) and data table evaluating conformations, additional gas sorption isotherms, and synchrotron PXRD patterns of PCN-39 from *in situ* measurements. See DOI: 10.1039/b000000x/

CCDC-950392, 950464, and 950465 contain the supplementary crystallographic data for this paper. These data can be obtained free of charge from The Cambridge Crystallographic Data Centre via www.ccdc.cam.ac.uk/data_request/cif.

View Article Online
DOI: 10.1039/C3TA12761C

1. H.-C. Zhou, J. R. Long and O. M. Yaghi, *Chem. Rev.*, 2012, **112**, 673-674.
2. O. M. Yaghi, M. O'Keeffe, N. W. Ockwig, H. K. Chae, M. Eddaoudi and J. Kim, *Nature*, 2003, **423**, 705-714.
3. D.-Y. Hong, Y. K. Hwang, C. Serre, G. Férey and J.-S. Chang, *Adv. Funct. Mater.*, 2009, **19**, 1537-1552.
4. S. Kitagawa, R. Kitaura and S.-i. Noro, *Angew. Chem. Int. Ed.*, 2004, **43**, 2334-2375.
5. J. J. Perry Iv, J. A. Perman and M. J. Zaworotko, *Chem. Soc. Rev.*, 2009, **38**, 1400-1417.
6. L. J. Murray, M. Dinca and J. R. Long, *Chem. Soc. Rev.*, 2009, **38**, 1294-1314.
7. A. G. Wong-Foy, A. J. Matzger and O. M. Yaghi, *J. Am. Chem. Soc.*, 2006, **128**, 3494-3495.
8. J. Sculley, D. Yuan and H.-C. Zhou, *Energy Environ. Sci.*, 2011, **4**, 2721-2735.
9. M. Dincă, A. Dailly, Y. Liu, C. M. Brown, D. A. Neumann and J. R. Long, *J. Am. Chem. Soc.*, 2006, **128**, 16876-16883.
10. J.-R. Li, Y. Ma, M. C. McCarthy, J. Sculley, J. Yu, H.-K. Jeong, P. B. Balbuena and H.-C. Zhou, *Coord. Chem. Rev.*, 2011, **255**, 1791-1823.
11. H. Furukawa, N. Ko, Y. B. Go, N. Aratani, S. B. Choi, E. Choi, A. Ö. Yazaydin, R. Q. Snurr, M. O'Keeffe, J. Kim and O. M. Yaghi, *Science*, 2010, **329**, 424-428.
12. O. K. Farha, A. O. Yazaydin, I. Eryazici, C. D. Malliakas, B. G. Hauser, M. G. Kanatzidis, S. T. Nguyen, R. Q. Snurr and J. T. Hupp, *Nat. Chem.*, 2010, **2**, 944-948.
13. J.-R. Li, J. Sculley and H.-C. Zhou, *Chem. Rev.*, 2012, **112**, 869-932.
14. H. Wu, Q. Gong, D. H. Olson and J. Li, *Chem. Rev.*, 2012, **112**, 836-868.
15. K. Sumida, D. L. Rogow, J. A. Mason, T. M. McDonald, E. D. Bloch, Z. R. Herm, T.-H. Bae and J. R. Long, *Chem. Rev.*, 2012, **112**, 724-781.
16. J.-R. Li, R. J. Kuppler and H.-C. Zhou, *Chem. Soc. Rev.*, 2009, **38**, 1477-1504.
17. Y. Liu, W. Xuan and Y. Cui, *Adv. Mater.*, 2010, **22**, 4112-4135.
18. J. Park, J.-R. Li, Y.-P. Chen, J. Yu, A. A. Yakovenko, Z. U. Wang, L.-B. Sun, P. B. Balbuena and H.-C. Zhou, *Chem. Commun.*, 2012, **48**, 9995-9997.
19. D. Feng, Z.-Y. Gu, J.-R. Li, H.-L. Jiang, Z. Wei and H.-C. Zhou, *Angew. Chem. Int. Ed.*, 2012, **51**, 10307-10310.
20. M. Padmanaban, P. Muller, C. Lieder, K. Gedrich, R. Grunker, V. Bon, I. Senkovska, S. Baumgartner, S. Opelt, S. Paasch, E. Brunner, F. Glorius, E. Klemm and S. Kaskel, *Chem. Commun.*, 2011, **47**, 12089-12091.
21. J. Lee, O. K. Farha, J. Roberts, K. A. Scheidt, S. T. Nguyen and J. T. Hupp, *Chem. Soc. Rev.*, 2009, **38**, 1450-1459.
22. L. Ma, C. Abney and W. Lin, *Chem. Soc. Rev.*, 2009, **38**, 1248-1256.
23. B. Chen, L. Wang, Y. Xiao, F. R. Fronczek, M. Xue, Y. Cui and G. Qian, *Angew. Chem. Int. Ed.*, 2009, **48**, 500-503.
24. B. Chen, L. Wang, F. Zapata, G. Qian and E. B. Lobkovsky, *J. Am. Chem. Soc.*, 2008, **130**, 6718-6719.
25. B. V. Harbuzaru, A. Corma, F. Rey, P. Atienzar, J. L. Jordá, H. García, D. Ananias, L. D. Carlos and J. Rocha, *Angew. Chem. Int. Ed.*, 2008, **47**, 1080-1083.
26. M. D. Allendorf, C. A. Bauer, R. K. Bhakta and R. J. T. Houk, *Chem. Soc. Rev.*, 2009, **38**, 1330-1352.
27. L. E. Kreno, K. Leong, O. K. Farha, M. Allendorf, R. P. Van Duyne and J. T. Hupp, *Chem. Rev.*, 2012, **112**, 1105-1125.
28. C. Gaudin, D. Cunha, E. Ivanoff, P. Horcajada, G. Cheve, A. Yasri, O. Loget, C. Serre and G. Maurin, *Microporous Mesoporous Mater.*, 2012, **157**, 124-130.
29. P. Horcajada, R. Gref, T. Baati, P. K. Allan, G. Maurin, P. Couvreur, G. Ferey, R. E. Morris and C. Serre, *Chem. Rev.*, 2012, **112**, 1232-1268.
30. M. Vallet-Regí, F. Balas and D. Arcos, *Angew. Chem. Int. Ed.*, 2007, **46**, 7548-7558.
31. J. Park, D. Yuan, K. T. Pham, J.-R. Li, A. Yakovenko and H.-C. Zhou, *J. Am. Chem. Soc.*, 2012, **134**, 99-102.
32. Q.-L. Zhu, T.-L. Sheng, R.-B. Fu, S.-M. Hu, L. Chen, C.-J. Shen, X. Ma and X.-T. Wu, *Chem. Eur. J.*, 2011, **17**, 3358-3362.
33. N. Yanai, T. Uemura, M. Inoue, R. Matsuda, T. Fukushima, M. Tsujimoto, S. Isoda and S. Kitagawa, *J. Am. Chem. Soc.*, 2012, **134**, 4501-4504.
34. S. J. Geier, J. A. Mason, E. D. Bloch, W. L. Queen, M. R. Hudson, C. M. Brown and J. R. Long, *Chem. Sci.*, 2013, **4**, 2054-2061.
35. E. D. Bloch, L. J. Murray, W. L. Queen, S. Chavan, S. N. Maximoff, J. P. Bigi, R. Krishna, V. K. Peterson, F. Grandjean, G. J. Long, B. Smit, S. Bordiga, C. M. Brown and J. R. Long, *J. Am. Chem. Soc.*, 2011, **133**, 14814-14822.
36. W. Yang, A. J. Davies, X. Lin, M. Suyetin, R. Matsuda, A. J. Blake, C. Wilson, W. Lewis, J. E. Parker, C. C. Tang, M. W. George, P. Hubberstey, S. Kitagawa, H. Sakamoto, E. Bichoutskaia, N. R. Champness, S. Yang and M. Schroder, *Chem. Sci.*, 2012, **3**, 2993-2999.
37. M. Dincă and J. R. Long, *J. Am. Chem. Soc.*, 2005, **127**, 9376-9377.
38. M. Eddaoudi, J. Kim, N. Rosi, D. Vodak, J. Wachter, M. O'Keeffe and O. M. Yaghi, *Science*, 2002, **295**, 469-472.
39. T. A. Makal, A. A. Yakovenko and H.-C. Zhou, *J. Phys. Chem. Lett.*, 2011, **2**, 1682-1689.
40. M. Dan-Hardi, H. Chevreau, T. Devic, P. Horcajada, G. Maurin, G. Ferey, D. Popov, C. Riekel, S. Wuttke, J. C. Lavalley, A. Vimont, T. Boudewijns, D. de Vos and C. Serre, *Chem. Mater.*, 2012, **24**, 2486-2492.
41. W. Zhuang, S. Ma, X.-S. Wang, D. Yuan, J.-R. Li, D. Zhao and H.-C. Zhou, *Chem. Commun.*, 2010, **46**, 5223-5225.
42. L. Hintermann, R. Masuo and K. Suzuki, *Org. Lett.*, 2008, **10**, 4859-4862.
43. G. Sheldrick, *Acta Crystallogr. Sect. A: Found. Crystallogr.*, 2008, **64**, 112-122.
44. A. Spek, *J. Appl. Cryst.*, 2003, **36**, 7-13.

View Article Online
DOI: 10.1039/C3TA12761E

45. K. S. W. Sing, D. H. Everett, R. A. W. Haul, L. Moscou, R. A. Pierotti, J. Rouquerol and T. Siemieniewska, *Pure Appl. Chem.*, 1985, **57**, 603-619.
46. O. K. Farha, K. L. Mulfort and J. T. Hupp, *Inorg. Chem.*, 2008, **47**, 10223-10225.
47. M. Fischer, F. Hoffmann and M. Froba, *RSC Advances*, 2012, **2**, 4382-4396.
48. M. Arif Nadeem, A. W. Thornton, M. R. Hill and J. A. Stride, *Dalton Trans.*, 2011, **40**, 3398-3401.